Role of the Support in Determining the Vibrational Properties of Carbonyls Formed on Pd Supported on SiO2Al2O3, Al2O3, and MgO

ARTICLE *in* THE JOURNAL OF PHYSICAL CHEMISTRY C · MAY 2007

Impact Factor: 4.77 · DOI: 10.1021/jp0666434

Role of the Support in Determining the Vibrational Properties of Carbonyls Formed on Pd Supported on $SiO_2-Al_2O_3$, Al_2O_3, and MgO

E. Groppo,[†] S. Bertarione,[†] F. Rotunno,[†] G. Agostini,[†] D. Scarano,[†] R. Pellegrini,[‡] G. Leofanti,[‡,§] A. Zecchina,[†] and C. Lamberti*[,†]

Department of Inorganic, Physical and Materials Chemistry, NIS Centre of Excellence, and Centro di Riferimento INSTM, University of Turin, Via P. Giuria 7, I-10125, Torino, Italy, Chimet SpA−Catalyst Division, Via di Pescaiola 74, Viciomaggio Arezzo, I-52040 Italy, Consultant, Via Firenze 43, 20010 Canegrate (Milano), Italy

Received: October 10, 2006; In Final Form: February 8, 2007

The vibrational properties of adsorbed carbonyls on heterogeneous Pd/oxide systems ($SiO_2-Al_2O_3$, Al_2O_3, and MgO) are compared and discussed. On the basis of the surface science literature, the complex IR spectra of carbonyls formed on Pd particles are interpreted in terms of what occurs on well-defined Pd(111) and Pd(100) faces and on edge/corner defects, typical of metal nanoparticles, thus bridging the gap between single crystals and high surface area systems. Furthermore, the influence of the electronic properties of the support (i.e., surface acidity/basicity) in determining the spectral features of carbonyls formed on Pd particles is clearly demonstrated.

1. Introduction

How different are surface science and catalysis, two branches of science that appear to be at the two opposite ends of the same logical line? The former applies to ideal systems (single crystals or films) where the investigated face is selected by the scientist before the experiment, resulting in the presence of one (or few) well-defined adsorption site(s).[1−16] The latter applies to high surface area systems characterized by an intrinsically large heterogeneity of exposed faces and thus of families of adsorbing sites, whose structure and relative population is, a priori, unknown.[17−25]

In principle, a systematic study of the most abundant surfaces with a surface science approach should give all the "simple" pieces of the large puzzle represented by the real catalytic system. Actually, this ambitious project may fail for three main reasons. (i) One may acquire pieces of different puzzles, as the experimental techniques (IRAS or HREELS vs transmission IR, limiting the list to vibrational techniques) and the thermodynamic conditions (temperature and equilibrium pressures) adopted in the surface science approach are largely different from those usually adopted in the investigation of high surface area materials. (ii) The final puzzle may contain a too large number of pieces to be acquired, assembled, or both. (iii) Some pieces of the puzzle may not be found (or can be present in a very low amount) in surface science experiments. This is the case of the defective sites (edges, corners, steps, etc.) and of the electronic effects induced by the support. These three limiting points explain why the gap between surface science and catalysis has been completely bridged only in a restricted number of cases.[23] This is the case, for example, for α-Cr_2O_3[26], NiO[27], and MgO.[24,28]

In this work, focused on the vibrational properties of adsorbed carbonyls, we will show that the gap between the single crystals and the polycrystalline systems can be bridged also in the case of Pd metal particles supported on high surface area inorganic oxides, namely, $SiO_2-Al_2O_3$, Al_2O_3, and MgO, which are important catalysts for selective hydrogenation reactions in the synthesis of both fine chemicals such as agrochemicals and pharmaceutical[29] and bulk chemical products.[30,31] This work complements the recent studies of Lear et al.[32,33] that investigate the CO adsorption on Pd nanoparticles prepared via five different precursors on an Al_2O_3 support.

In order to reach the same thermodynamic conditions (CO coverage, hereafter θ) of the surface science experiments performed on Pd single crystals, it has been necessary to adopt for the Pd/oxide systems an ad hoc designed approach; it will be discussed in the following paragraphs. This experimental procedure allows us to avoid problems related to the first point (i) outlined above, that is, to collect pieces belonging to the same puzzle. Starting from this basis, the complex IR spectra of CO adsorbed on heterogeneous Pd/oxide systems will be fully explained in terms of what occurs on well-defined Pd(111) and Pd(100) faces. Of course, the situation will result in a problem more complex than that investigated on single crystals for the difficulties related to the second and third points (ii and iii) that are intrinsically unavoidable. In this peculiar case, the spectra result from the overlap of the vibrational features of the carbonyl species adsorbed on both Pd(111) and Pd(100) faces. Furthermore, the presence of at least two families of adsorbing sites characterized by slightly different local environments, such as sites in the middle of the faces and sites closed to the edges and corners, has to be considered. Finally, the vibrational properties of the carbonyls formed on Pd particles are strongly influenced by a transfer of electron density between the support and the Pd particles. This means that Pd particles with very similar morphology on supports characterized by a different electronic behavior (i.e., a different acidity/basicity) may show different carbonyl features.

* Corresponding author. Fax: +39011-6707855. E-mail: carlo.lamberti@unito.it.
[†] University of Turin.
[‡] Chimet SpA.
[§] Consultant.

10.1021/jp0666434 CCC: $37.00
Published on Web 04/24/2007

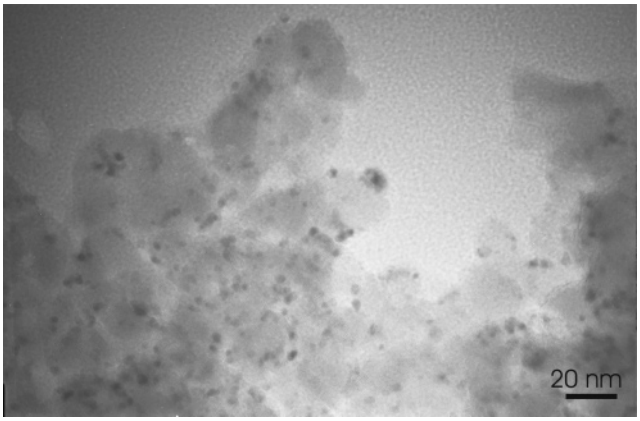

Figure 1. TEM micrograph of the $Pd/SiO_2-Al_2O_3$ sample. Only a few particles with an average diameter in the 1.5−3.0 nm range are visible, whereas the majority of Pd is not detected, as a consequence of the too small particle size.

2. Experimental Section

$Pd/SiO_2-Al_2O_3$ and Pd/Al_2O_3 samples have been prepared in the Chimet laboratories by supporting 2 wt% of Pd from Na_2PdCl_4 on $SiO_2-Al_2O_3$ (Si/Al = 5.7; surface area = 180 m^2 g^{-1}) and Al_2O_3 (surface area = 170 m^2 g^{-1}) supports. The two samples have been reduced at 673 K in H_2 atmosphere. CO chemisorption measurements, performed with a Micromeritics Autochem 2910 instrument, gave a dispersion, defined as the ratio between the number of adsorbed CO molecules and the number of Pd atoms, of 0.23 and 0.27, for $Pd/SiO_2-Al_2O_3$ and Pd/Al_2O_3 samples, respectively. The high dispersion is confirmed by TEM analysis, performed using a Jeol 2000 EX instrument equipped with a top-entry stage and operating at 200 kV. Figure 1 reports a micrograph of the $Pd/SiO_2-Al_2O_3$ sample (a similar image is obtained for Pd/Al_2O_3, not shown for brevity), showing only a few particles with an average diameter in the 1.5−3.0 nm range, whereas the majority of Pd is not visible because of a smaller particle size (lower than 1.0 nm).

In order to investigate the effect of support basicity, we have also prepared a 10 wt% Pd/MgO sample by wet impregnation of $Mg(OH)_2$ with a solution of $[Pd(NH_3)_4](NO_3)_2$. This sample has been dried overnight and then reduced at 623 K in H_2 atmosphere. Under these conditions, $Mg(OH)_2$ looses water resulting in high surface area (230 m^2 g^{-1}) MgO.[24] The Pd/MgO sample is characterized by the presence of Pd particle aggregates with dimensions in the 60−90 nm range.[10] However, Fourier transform infrared (FTIR) spectroscopy of adsorbed CO, which is the technique used in this study, is much more sensitive toward the fraction of the Pd particles with a smaller size, that is, those particles presenting a much higher surface area.

The IR experiments have been performed on self-supported pellets inside an IR quartz cell allowing in situ thermal treatments and gas dosages to be done. The sample has been heated up to 673 K under dynamical vacuum, followed by a reduction process consisting of three subsequent H_2 dosages (equilibrium pressure P_{H_2} = 120 Torr, 1 Torr = 133.3 Pa, contact time = 5 min). After the last H_2 removal at 673 K down to $P_{H_2} < 10^{-4}$ Torr, the sample has been cooled down to 300 K in dynamical vacuum. The FTIR spectra were recorded at 300 K at 2 cm^{-1} resolution, using a Bruker IFS 28 spectrometer, equipped with a cryogenic MCT detector.

All of the spectra reported in the work have been normalized in order to take into account the different optical thicknesses of the samples, that is, the quantity of Pd crossed by the IR beam. Consequently, along the whole set of samples, the apparent intensity of a given band is directly proportional to the amount of carbonyl species responsible for the component, so that all of the spectra are directly comparable. The real absorbance value of the more intense component in all of the figures is reported in the relative caption, in order to give an idea of the signal-to-noise ratio.

3. Results and Discussion

3.1. Brief Overview of Surface Science Results. Vibrational spectroscopies, both infrared reflection absorption spectroscopy (IRAS) and high-resolution electron energy-loss spectroscopy (HREELS), of adsorbed CO have been widely employed to characterize vacuum cleaved Pd(*hkl*) single-crystal surfaces.[1−11,34] Three main categories of carbonyls can be identified, which are characterized by rather defined frequency regions for the C−O stretching mode:[9,35,36] (i) linear carbonyls (on-top sites) usually absorb in the ∼2130−2000 cm^{-1} stretching region; (ii) twofold bridged carbonyls are characterized by a $\tilde{\nu}$(C−O) in the ∼2000−1850 cm^{-1} interval; and (iii) threefold bridged carbonyls (on hollow sites) are defined by a C−O stretching mode in the ∼1920−1800 cm^{-1} region. In all cases, we are dealing with classical carbonyls, where the π back-donation effects, causing a red shift of the $\tilde{\nu}$(C−O), are largely dominant with respect to the σ donation and electrostatic effects, both contributing to a blue shift of the $\tilde{\nu}$(C−O).[37−39] The frequency ranges of linear, twofold, and threefold bridged carbonyls reported above are quite large as different phenomena influence the observed $\tilde{\nu}$(C−O). Because of the progressive building up of lateral−lateral interactions among adsorbed CO molecules, the C−O stretching frequencies of linear and bridged carbonyls show important blue shifts upon increasing θ,[11,40−43] hereafter given in CO monolayers. It is worth to note that the exact frequency interval of the three categories of carbonyls, as well as the precise $\tilde{\nu}$(C−O) versus θ evolution, may slightly change as a function of the experimental conditions (temperature, equilibrium pressure, etc.) and from author to author.[1−12,34,40] This incertitude, basically focused on the precise location of the threefold-to-twofold transition, will result in two possible interpretations of the high coverage spectra obtained on powdered samples, vide infra section 3.2.2.

As far as the Pd(111) surface is concerned, the evolution versus θ of the IRAS spectra measured upon dosing CO can be summarized as follows. (i) At the lowest θ, only threefold bridged carbonyls are observed, at a distinctly low $\tilde{\nu}$(C−O) around 1810 cm^{-1}.[11,40,41] (ii) Increasing θ up to ∼0.5, it has been suggested that CO molecules occupy either twofold bridging sites or threefold hollow sites. This structure is essentially characterized by a band around 1920 cm^{-1}.[11] (iii) Within θ = 0.5−0.7, various complex overlayer structures have been reported.[11,34,40] In particular, around θ = 0.7, it has been suggested that some CO molecules are forced into top sites with a simultaneous reconstruction of the twofold structure, resulting into a shift of the twofold band up to 1946 cm^{-1} and into the contemporaneous appearance of a band around 2080 cm^{-1}, due to linear carbonyls.[40] (iv) A further increase of θ results in a progressive strength of these two last components that simultaneously shift upward to 1952 and 2090 cm^{-1}, respectively.[11] It is worth noticing that at these θ values a small component around 2090 cm^{-1} is often present in the IRAS spectra (see, e.g., Figures 1 and 2 in ref 41 or Figure 2a in ref 11), even if it is rarely discussed. This component, clearly in the region of linear carbonyls, can be assigned to carbonyls formed on a small fraction of defects. (v) At maximum coverage ($\theta \geq 0.75$), a new surface rearrangement occurs, resulting in a complex

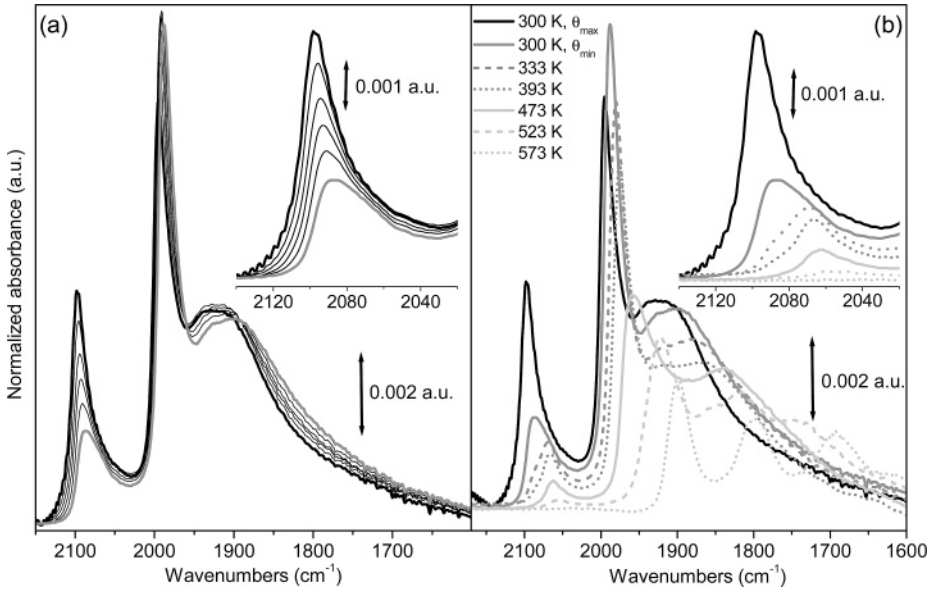

Figure 2. (a) FTIR spectra, in the CO stretching region, of CO dosed at 300 K on $Pd/SiO_2-Al_2O_3$, previously reduced at 673 K, upon decreasing θ at 300 K, from $P_{CO} = 50$ Torr (bold black spectrum) to $P_{CO} = 10^{-4}$ Torr (bold gray spectrum). (b) Successive desorption steps at increasing temperatures (see legend). In both part a and part b, the insets report a magnification of the 2120−2040 cm^{-1} region, due to linear carbonyls. The vertical axis reports the absorbance normalized to the optical thickness of the sample (74.6 mg/cm^2). The band at 1994 cm^{-1} at θ_{max} (bold black spectrum) has an absorbance of 0.73 in the original spectrum.

evolution of the CO spectra,[11] which is not discussed here as we have never reached such a high coverage in the IR experiments of CO dosed on the Pd-supported catalysts investigated in this work.

A much simpler spectral evolution has been observed upon increasing θ on the Pd(100) face.[11] In this case, only twofold bridged carbonyl species have been observed whose $\tilde{\nu}$(C−O) moves from 1895 cm^{-1} ($\theta \approx 0.05$) up to 1995 cm^{-1} at θ_{max}.[11,44]

3.2. IR Spectra of CO Adsorbed on $Pd/SiO_2-Al_2O_3$. *3.2.1. CO Coverage Tuned by Room Temperature Evacuation.* Figure 2a reports the IR spectra of CO dosed at 300 K on $Pd/SiO_2-Al_2O_3$, previously reduced at 673 K in H_2, upon decreasing θ. Within our experimental conditions, θ_{max} (bold black curve) corresponds to $T = 300$ K and $P_{CO} = 50$ Torr, whereas θ_{min} (bold dark gray curve) is obtained by evacuation at 300 K down to 10^{-4} Torr. Three components are clearly visible in this set of spectra. (i) The high-frequency component progressively decreases in intensity and moves from 2097 to 2087 cm^{-1} ($|\Delta\tilde{\nu}| = 10$ cm^{-1}) upon lowering θ. The high θ_{max} spectrum presents a tail at the low-frequency side, which progressively becomes relatively more relevant upon lowering θ. Both bands are in the range of linear carbonyls, but show a marked different behavior. The low-frequency shoulder is coverage independent, in both intensity and frequency in this θ range; on this basis, it is ascribed to CO linearly adsorbed on defects.[11,45] Conversely, the important blue shift characterizing the band dominating the θ_{max} spectrum ($|\Delta\tilde{\nu}| = 10$ cm^{-1}) makes difficult its assignment to linear carbonyls adsorbed on defects (as advanced by Lear et al.[32,33]) and favors its interpretation in terms of linear CO molecules adsorbed on well-defined Pd(111) faces. (ii) The most intense and sharp band of the whole set of spectra moves from 1994 cm^{-1} down to 1988 cm^{-1} ($|\Delta\tilde{\nu}| = 6$ cm^{-1}) upon reducing P_{CO}, accompanied by a slight intensity increase. (iii) Finally, a broad component centered at θ_{max} around 1925 cm^{-1} progressively shifts downward to 1905 cm^{-1} at θ_{min} ($|\Delta\tilde{\nu}| = 20$ cm^{-1}). Component (ii) clearly lies in the range where twofold bridged carbonyls on Pd(100) are expected, while component (iii) lies in the region of overlap between twofold and threefold bridged carbonyls on Pd(111), and its assignment is less straightforward.

The three main components characterizing the spectra reported in Figure 2a exhibit a frequency shift much smaller than that investigated in the single-crystal experiments summarized in section 3.1. Moreover, no evidence of threefold carbonyls below 1900 cm^{-1} is detectable. These observations suggest that, in the thermodynamic conditions reached in the experiment reported in Figure 2a, we are unable to reach, by far, a θ_{min} comparable to that reached in the ultra high vacuum (UHV) conditions of the single-crystal experiments. For this reason, a complete assignment of spectral components to different carbonyl species is not possible at this stage.

3.2.2. Temperature Programmed IR Desorption Study: A Way to Reach Low CO Coverage Comparable with Surface Science Results. To be able to compare our IR data with the surface science literature, that is, to reach lower θ values, the desorption process was progressively performed (down to $P_{CO} = 10^{-4}$ Torr) at increasing temperatures, up to 573 K. The IR spectra obtained in such conditions are reported in Figure 2b. As done for the literature data on single crystals discussed in section 3.1., we will present the spectra reported in Figure 2b as a function of increasing θ.

The lowest θ spectrum (dotted light gray curve in Figure 2b) exhibits three main components, at 1900, 1800, and 1694 cm^{-1}. The two bands at 1900 and 1800 cm^{-1} can be attributed straightforwardly to twofold bridged carbonyls on Pd(100) faces ($\tilde{\nu}$(C−O) = 1895 cm^{-1} on single crystals) and to threefold bridged carbonyls on Pd(111) faces ($\tilde{\nu}$(C−O) = 1807 cm^{-1} on single crystals), respectively.[11,40] The θ value reached by CO desorption at 573 K is sufficiently low to guarantee the absence of any feature due to linear carbonyls on well-defined faces ($\theta < 0.6$ according to single-crystal literature).[11] As for the component at 1694 cm^{-1}, which is an extremely low frequency and never observed on single crystals, it will be discussed separately at the end of this section.

Upon increasing θ, the 1900 cm^{-1} component, due to the twofold bridged carbonyls on Pd(100) faces, progressively shifts upward at 1922, 1958, 1976, 1981, and up to 1988 cm^{-1}, for the spectrum collected after CO evacuation at 300 K (bold gray spectrum in Figure 2b). The value measured at $P_{CO} = 50$ Torr,

TABLE 1: $\tilde{\nu}$(C−O) (in cm^{-1}) of the Different Type of Carbonyls Formed on Pd(111) and Pd(100) Faces of Pd/SiO_2−Al_2O_3 at Different Coverage[a]

	Pd(111)			Pd(100)	defects
desorption T (K)	threefold	twofold	linear	twofold	linear
573	1800			1900	
523	1820			1922	
473	1841			1958	2064
393	1865			1976	2066
333	1880		*2087* (sh)	1981	2067
300 (10^{-4} Torr)		*1905*	*2087*	1988	nr
300 (θ_{max})		*1925*	*2097*	1994	nr

[a] Coverage expressed in terms of desorption temperature. The frequency values refer to Figure 2. sh = shoulder, nr = not resolved. Bands whose frequencies are written in italics may be interpreted according to an alternative interpretation (see text for details): bands in the column of twofold bridged carbonyls on Pd(111) can be attributed to threefold bridged carbonyls on the same face, while bands in the column of linear carbonyls on Pd(111) can be attributed to linear carbonyls formed on defects.

$\tilde{\nu}$(C−O) = 1994 cm^{-1}, exactly corresponds to the frequency observed on single-crystal Pd(100) faces at θ_{max}.[11,40]

The evolution of the 1800 cm^{-1} component, due to threefold bridged carbonyls on Pd(111) faces, is more complex (see Table 1). A progressive θ increase results in an upward shift to 1820, 1841, 1865, 1880, and up to 1905 cm^{-1} in the sample desorbed at 300 K (Table 1 and Figure 2b). All of these bands are characterized by a high energy shoulder, that could be explained in terms of surface heterogeneity. Starting from the sample desorbed at 473 K, we find that a contribution in the region of linear carbonyls gradually appears. This absorption, initially centered at 2064 cm^{-1} (sample desorbed at 473 K, full light gray curve in Figure 2b), splits into two components upon increasing θ. The low-frequency component, more important at low θ, is almost coverage-independent in frequency (appearing at 2067 cm^{-1} in the sample desorbed at 333 K, dashed gray curve) and rapidly saturates in intensity. Conversely, the high-frequency component becomes the dominant one in the θ region discussed in Figure 2a and undergoes an upward shift of +10 cm^{-1} (passing from 2087 to 2097 cm^{-1}, see Table 1). As it is advanced at the end of section 3.2.1., the frequency evolution of these two components confirms their attribution to linear carbonyls adsorbed on defects (low-frequency) and on Pd(111) faces (high-frequency). Coming to the intensities, care must be taken in correlating their integrated area at θ_{max} to their relative abundance. As clearly reviewed in the work of Hollins,[45] the high-frequency component can gain intensity due to a "coupling interaction" within CO adlayers, because of a characteristic transfer of intensity occurring from the band due to lower-frequency species (linear CO on defects) to that of its high-frequency counterpart (CO on well-defined Pd faces). This transfer is particularly efficient when the frequency separation is small.[45,46]

The assignment of the linear carbonyl bands reported above has consequences on the interpretation of the bands of bridged carbonyls on the Pd(111) face. According to the surface science literature, linear carbonyls on Pd(111) faces start to appear around θ = 0.7, accompanied by the presence of twofold bridged carbonyls on the same face.[11,34,40] For this reason, the component moving in the RT desorption experiment from 1925 to 1905 cm^{-1} should be attributed to twofold bridged carbonyls on the Pd(111) face (Table 1). This implies that, upon increasing θ, the threefold bridged carbonyls persist until linear carbonyls appear; at this point, they are converted into twofold bridged carbonyls due to a surface rearrangement (sample desorbed at 300 K, full gray curve in Figure 2b).

However, it is well-known that the 1925−1905 cm^{-1} interval lies in the frequency frontier between the regions of three- and twofold bridged carbonyls and that the bands falling there have been assigned to both species moving from author to author of the quoted literature. The nonstraightforward assignment of the band in the 1925−1905 cm^{-1} interval to twofold bridged carbonyls, in turn, makes questionable the assignment of the highest $\tilde{\nu}$(C−O) to linear carbonyls on Pd(111). In the case that all of the components appearing in the 1925−1905 cm^{-1} interval are assigned to threefold bridged carbonyls on Pd(111), that is, we assume that the θ value reached in our experiment does not allow the threefold-to-twofold plus linear surface rearrangement on Pd(111) faces, than the two families of bands observed in the linear carbonyl regions have to be assigned to CO adsorbed on two different types of defects (steps and corners). As already recalled, this is the assignment made by Lear et al.[32,33] Notwithstanding this alternative interpretation simplifies the assignments of the bands in the bridged carbonyls region, it has serious difficulties in explaining both the magnitude and the sign of the shift undergone by the high-frequency component upon increasing θ: $\Delta\tilde{\nu} = \tilde{\nu}(\theta_{max}) - \tilde{\nu}(\theta_{min}) = 10$ cm^{-1}.

Summarizing, the surface science literature allows us to (i) give a straightforward interpretation of the low θ spectra in terms of two- and threefold bridged carbonyls adsorbed on Pd(100) and Pd(111) faces, respectively, and (ii) advance two alternative interpretations (both having different strengths and weaknesses) of the high θ spectra.

Returning now to the third component characterizing the lowest θ spectrum (dotted light gray curve in Figure 2b), we find that its frequency (1694 cm^{-1}) is extremely low to allow an assignment in terms of a standard carbonyl species.[11,40,45] An easy explanation for this band can be found by claiming the formation of carbonates during the CO desorption procedure at increasing temperature. Disproportionation of CO with the formation of CO_2 and thus of carbonates occurs at relatively low temperatures on several Pd-supported systems.[47−49] However, the band at 1694 cm^{-1} rapidly disappears when 50 Torr of CO are dosed again on the system subjected to the thermal desorption procedure, as reported in Figure 3 (evolution from the dotted light gray to the dotted black curve). The spectrum obtained in these conditions (dotted black curve) shows no more features around 1700 cm^{-1}, suggesting that the species responsible for this band are displaced by the incoming CO molecules and thus are not stable species. This observation directly excludes the assignment of the band at 1694 cm^{-1} to carbonate species, even if a small disproportionation of CO with the consequent poisoning of the Pd surface cannot be completely ruled out. The small decrease of the intensity of the overall spectrum and the downward shift of all of the components with respect to the starting CO spectrum (full black line in Figure 3) is reflecting, indeed, the fact that, at the same P_{CO}, a slightly lower θ value is obtained when CO is dosed again on the sample after the thermal desorption procedure.[50]

By excluding the assignment in terms of the carbonate species, the band at 1694 cm^{-1} must be interpreted in terms of a highly perturbed carbonyl. It is well-known that CO groups in metal carbonyls exhibit a distinct basicity at the carbonyl oxygen.[21,51−53] For this reason, in the presence of a Lewis acid site, an O-bonded σ adduct can be formed, which is characterized by a significant decrease of the CO stretching frequency.[21,54,55] Carbonyl adducts formed through more basic bridging CO groups are known to form stronger donor−acceptor

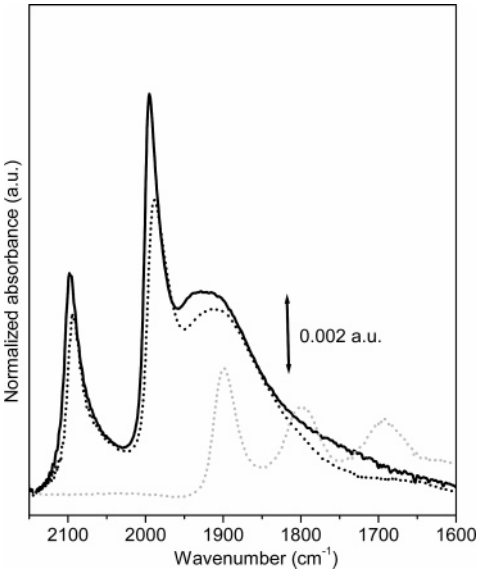

Figure 3. Effect of dosing again CO (dotted black curve) on the Pd/$SiO_2-Al_2O_3$ system subjected to the thermal desorption reported in Figure 2b. Bold black and dotted light gray curves as in Figure 2b. The vertical axis reports the absorbance normalized to the optical thickness of the sample (74.6 mg/cm^2). The band at 1994 cm^{-1} at θ_{max} (bold black spectrum) has an absorbance of 0.73 in the original spectrum.

bonds than those involving terminal CO ligands. Correspondingly, the CO vibrational spectrum is strongly perturbed, resulting in downward shifts of 100−150 cm^{-1} and 200−400 cm^{-1} for linear and bridging CO groups, respectively.[21,52,53,56] In view of this fact and of the presence of strong Al^{3+} Lewis acid sites on the $SiO_2-Al_2O_3$ surface, the band at 1694 cm^{-1} characterizing the lowest θ spectrum in Figure 3 (dotted light gray curve) can be interpreted as being caused by a fraction of threefold bridged carbonyls interacting through the O termination with the Al^{3+} acid sites of the support. Increasing θ will result in the progressive population of adjacent threefold bridged carbonyls, with the parallel increase of lateral−lateral interactions destroying the interaction with the adjacent Al^{3+} support site. This explanation accounts for the upward shift of the band at 1694 cm^{-1} and up to 1740 cm^{-1} in the spectrum collected after desorption at 523 K (dashed light gray curve in Figure 3).

3.3. IR Spectra of CO Adsorbed on Pd/Al_2O_3. To understand the role of the support in determining the vibrational features of carbonyls formed on Pd particles, that is, (a) to identify the characteristics common to all supported Pd systems, differentiating them from Pd single crystals and (b) to point out which are the specific features conferred by each support, we have repeated the same experiment reported in Figure 2 on a Pd/Al_2O_3 (Figure 4) and Pd/MgO (see section 3.4. and Figure 5) samples. This plan is aimed to understand similarities and differences of the pieces of the different puzzles discussed in the Introduction.

As far as Pd/Al_2O_3 is concerned, the spectrum obtained at θ_{max} and at 300 K (bold black curve in Figure 4a) is characterized, as in the case of Pd/$SiO_2-Al_2O_3$, by three main components, at 2090, 1980, and 1930 cm^{-1}. Analogously to what was discussed in the case of Pd/$SiO_2-Al_2O_3$ (section 3.2.), the band at 1980 cm^{-1} is straightforwardly assigned to twofold carbonyls on Pd(100) faces, while the two bands at 2090 and 1930 cm^{-1} can be interpreted in two alternative ways. By following the first interpretation, they can be attributed to twofold (1930 cm^{-1}) and linear (2090 cm^{-1}) carbonyls on the Pd(111) surface. According to the second interpretation, they could be interpreted in terms of threefold carbonyls on Pd(111) and linear carbonyls on defects, respectively. The component in the linear carbonyls region is the only one to shift significantly upon CO desorption at 300 K ($|\Delta\tilde{\nu}| = 10$ cm^{-1}: bold gray curve in Figure 4a and Table 2). At θ_{min}, this absorption is clearly composed of two different components (2080 and 2063 cm^{-1}); the low-frequency one is certainly due to defects.

Also, the evolution of the spectra upon desorption at increasing temperature (Figure 4b) reflects what was already discussed in the case of Pd/$SiO_2-Al_2O_3$. In the case of Pd/Al_2O_3, however, bridged carbonyls result in well-defined components only for the lowest θ spectra (CO desorbed at 573 and 523 K, dotted and dashed light gray curves). At higher θ, the envelope of the bridged carbonyl bands is hugely tailed at the low-frequency side and does not allow an exact identification of the position of the two- and/or threefold carbonyls on the Pd(111) face, that are almost overshadowed by the well-defined dominating band due to twofold carbonyls on Pd(100). As a consequence, the evolution of the threefold carbonyls on Pd(111) faces into twofold ones, if present, is less defined than in the previous case (see Table 2).

The analogy between the Pd/Al_2O_3 and the Pd/$SiO_2-Al_2O_3$ carbonyls (compare Figure 4 with Figure 2) suggests that the Pd particles on the two supports have a similar morphology. However, the different components of the spectra present a different relative intensity, and the frequency values of all of the carbonyl species as a function of θ are, in general, slightly lower in the case of Pd/Al_2O_3 with respect to Pd/$SiO_2-Al_2O_3$ (compare Table 2 with Table 1). The different intensity ratio reflects a different proportion between Pd(111) and Pd(100) faces. Conversely, the lower-frequency values should be a consequence of the different electronic behavior of the two supports,[25] as it will be discussed in section 3.5. An important difference between spectra of Pd supported on $SiO_2-Al_2O_3$ and that supported on Al_2O_3 is the absence on the latter ones of the lowest frequency band at 1694 cm^{-1} in the lowest θ spectrum, corresponding to a desorption temperature of 573 K (dotted light gray curve in Figure 4b). Also this feature will be explained in section 3.5 in terms of a support effect.

3.4. IR Spectra of CO Adsorbed on Pd/MgO. The Pd particles supported on MgO show a morphology similar to that of Pd supported on $SiO_2-Al_2O_3$ and Al_2O_3, as demonstrated by the θ_{max} spectrum at 300 K (bold black curve in Figure 5a). The three main components assigned to twofold bridged and linear carbonyls on Pd(111) (or to threefold bridged carbonyls on Pd(111) and to linear carbonyls on defects) and to twofold carbonyls on Pd(100) are clearly recognizable, even if less intense, much broader, and shifted to lower frequencies with respect to the other two cases. Upon CO desorption at increasing temperatures (Figure 5b and Table 3), the three main bands show the behavior already discussed for Pd/$SiO_2-Al_2O_3$ and Pd/Al_2O_3, resulting at the lowest θ value (desorption at 523 K, light gray dashed curve in Figure 5b) in only two components at 1870 and 1796 cm^{-1}, due to twofold carbonyls on Pd(100) and threefold carbonyls on Pd(111), respectively. Note that the narrow band at 1665 cm^{-1}, present in all of the spectra, is due to surface carbonates formed upon disproportionation of CO on the highly basic MgO support.[10,18,57,58]

3.5. Role of the Support in Determining the Spectral Features of Carbonyls Formed on Pd Particles. Figure 6 compares the θ_{max} ($P_{CO} = 50$ Torr) and θ_{min} ($P_{CO} = 10^{-4}$ Torr after desorption at the highest temperature) spectra of the Pd/$SiO_2-Al_2O_3$, Pd/Al_2O_3, and Pd/MgO systems (black, dark gray, and light gray curves, respectively) discussed in the previous

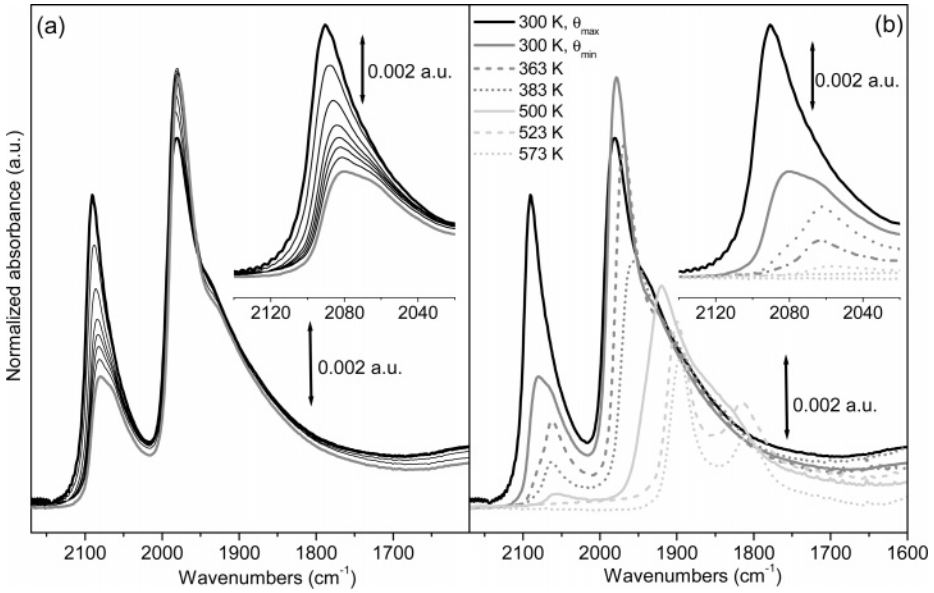

Figure 4. (a) FTIR spectra, in the CO stretching region, of CO dosed at 300 K on Pd/Al_2O_3 previously reduced at 673 K, upon decreasing θ at 300 K, from $P_{CO} = 50$ Torr (bold black spectrum) to $P_{CO} = 10^{-4}$ Torr (bold gray spectrum). (b) Successive desorption steps at increasing temperatures (see legend). In both part a and part b, the insets report a magnification of the 2120−2040 cm^{-1} region, due to linear carbonyls. The vertical axis reports the absorbance normalized to the optical thickness of the sample (26.3 mg/cm^2). The band at 1980 cm^{-1} at θ_{max} (bold black spectrum) has an absorbance of 0.23 in the original spectrum.

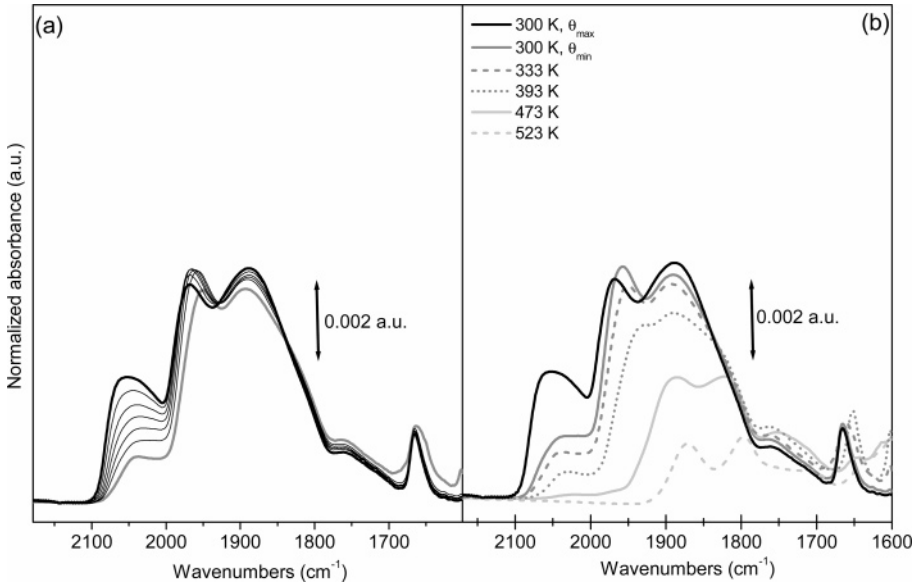

Figure 5. (a) FTIR spectra, in the CO stretching region, of CO dosed at 300 K on Pd/MgO previously reduced at 623 K, upon decreasing θ at 300 K, from $P_{CO} = 50$ Torr (bold black spectrum) to $P_{CO} = 10^{-4}$ Torr (bold gray spectrum). (b) Successive desorption steps at increasing temperatures (see legend). The vertical axis reports the absorbance normalized to the optical thickness of the sample (41.6 mg/cm^2). The band at 1970 cm^{-1} at θ_{max} (bold black spectrum) has an absorbance of 0.22 in the original spectrum.

sections and demonstrates that the support plays an important role in determining the vibrational properties of the carbonyls formed on Pd particles. As anticipated above, the Pd particles on the three systems are characterized by a similar morphology and exhibit mainly Pd(100) and Pd(111) faces. However, the θ_{max} spectra show a different intensity ratio between the three main components and show different frequency values (see Table 4 for comparison). The differences in the relative intensities of the main components suggest a different proportion between Pd(111) and Pd(100) faces in the three investigated systems. Conversely, the different frequencies should be a consequence of the different electronic behavior of the three supports. The decreasing of the $\tilde{\nu}$(C−O) by passing from $Pd/SiO_2-Al_2O_3$ to Pd/Al_2O_3 and to Pd/MgO samples (Table 4) are consistent with an increase in the back-donation of metal electrons into the antibonding CO $2\pi^*$ orbital.[25,59] This can be explained by considering that the basicity of the O atoms of the supports increases in the order $Pd/SiO_2-Al_2O_3 < Pd/Al_2O_3 \ll$ Pd/MgO. Much more basic are the O of the support, much more electron density is added to the Pd particles, thus increasing their ability to back-donate electron density to the adsorbed CO molecules, resulting in an increased red shift of the C−O stretching frequency.[37−39] The much higher basicity of the MgO support is indirectly demonstrated by the instantaneous formation of carbonate species upon CO dosage at 300 K (see the narrow band at 1665 cm^{-1} in Figure 5).

The observation that the spectral features of carbonyls formed on Pd particles are strongly dependent upon the electronic properties of the support is further supported by comparing the θ_{min} ($P_{CO} = 10^{-4}$ Torr after desorption at the highest temper-

TABLE 2: $\tilde{\nu}$(C−O) (in cm^{-1}) of the Different Type of Carbonyls Formed on Pd(111) and Pd(100) Faces of Pd/Al_2O_3 at Different Coverage[a]

	Pd(111)			Pd(100)	defects
desorption T (K)	threefold	twofold	linear	twofold	linear
573	1810			1895	
523	1816			1900	
500	1848			1920	2060
383	1911			1957	2062
363	1924			1968	2063
300 (10^{-4} Torr)		*1930*	*2080*	1978	2063 (sh)
300 (θ_{max})		*1930*	*2090*	1980	nr

[a] Coverage expressed in terms of desorption temperature. The frequency values refer to Figure 4. sh = shoulder, nr= not resolved. Bands whose frequencies are written in italics may be interpreted according to an alternative interpretation (see text for details): bands in the column of twofold bridged carbonyls on Pd(111) can be attributed to threefold bridged carbonyls on the same face, while bands in the column of linear carbonyls on Pd(111) can be attributed to linear carbonyls formed on defects.

TABLE 3: $\tilde{\nu}$(C−O) (in cm^{-1}) of the Different Type of Carbonyls Formed on Pd(111) and Pd(100) Faces of Pd/MgO at Different Coverage[a]

	Pd(111)			Pd(100)	defects
desorption T (K)	threefold	twofold	linear	twofold	linear
523	1796			1870	
473	1822			1888	
393	1887, 1840(sh)			1931	2032 (br)
333	1889			1950	2032 (br)
300 (10^{-4} Torr)		*1889*	*2042* (br)	1956	nr
300 (θ_{max})		*1889*	*2055* (br)	1970	nr

[a] Coverage expressed in terms of desorption temperature. The frequency values refer to Figure 5. sh = shoulder, br = broad, nr= not resolved. Bands whose frequencies are written in italics may be interpreted according to an alternative interpretation (see text for details): bands in the column of twofold bridged carbonyls on Pd(111) can be attributed to threefold bridged carbonyls on the same face, while bands in the column of linear carbonyls on Pd(111) can be attributed to linear carbonyls formed on defects.

ature) spectra of the Pd/SiO_2−Al_2O_3, Pd/Al_2O_3, and Pd/MgO systems (Figure 6b and Table 4). As it is observed for the carbonyl bands at θ_{max}, the two bands due to twofold carbonyls

TABLE 4: $\tilde{\nu}$(C−O) (in cm^{-1}) of the Different Type of Carbonyls Formed on Pd(111) and Pd(100) Faces at θ_{max} (P_{CO} = 50 Torr) and θ_{min} (P_{CO} = 10^{-4} Torr after Desorption at the Highest Temperature) on Different Pd-Supported Systems[a]

	Pd/SiO_2-Al_2O_3		Pd/Al_2O_3		Pd/MgO	
carbonyl type	θ_{max}	θ_{min}	θ_{max}	θ_{min}	θ_{max}	θ_{min}
linear (111)	*2097*		*2090*		*2055*	
twofold (100)	1994	1900	1980	1895	1970	1870
twofold (111)	*1925*		*1930*		*1889*	
threefold (111)		1800		1810		1796

[a] Frequency values refer to Figure 6. Bands whose frequencies are written in italics may be interpreted according to an alternative interpretation (see text for details): bands in the row of twofold bridged carbonyls on Pd(111) can be attributed to threefold bridged carbonyls on the same face, while bands in the row of linear carbonyls on Pd(111) can be attributed to linear carbonyls formed on defects.

on Pd(100) and threefold carbonyls on Pd(111) are occurring at lower frequencies with the increase of the support basicity. Furthermore, only the Pd/SiO_2−Al_2O_3 sample presents a band around 1700 cm^{-1}, which has been assigned to a fraction of threefold bridged carbonyls interacting through the O termination with the Al^{3+} acid sites of the support (vide supra section 3.2.2.). The absence of this component in the θ_{min} spectra of Pd/Al_2O_3 and Pd/MgO systems is a further proof of the higher basicity of the pure Al_2O_3 and MgO supports with respect to the SiO_2−Al_2O_3 one. In other words, the bridged carbonyls remaining on Pd/Al_2O_3 and Pd/MgO after the desorption process at increasing temperature do not find highly acid sites, as it happens for those present on the Pd/SiO_2−Al_2O_3.

The interpretation of the CO stretching frequencies reported so far is focused on the different acidity/basicity of the supports. This concept includes both the nature of the support itself and the effect that anions/cations of the Pd precursor may have in determining the overall electron transfer ability of the system toward adsorbed CO molecules. This is particularly relevant when chlorine containing precursors are used (Pd/SiO_2−Al_2O_3 and Pd/Al_2O_3 in our case). It is known, in fact, that they can leave residues both on the support and on the Pd nanoparticles,[32,33] which, of course, influence the adsorption properties of the entire system. In particular, it has been demonstrated that

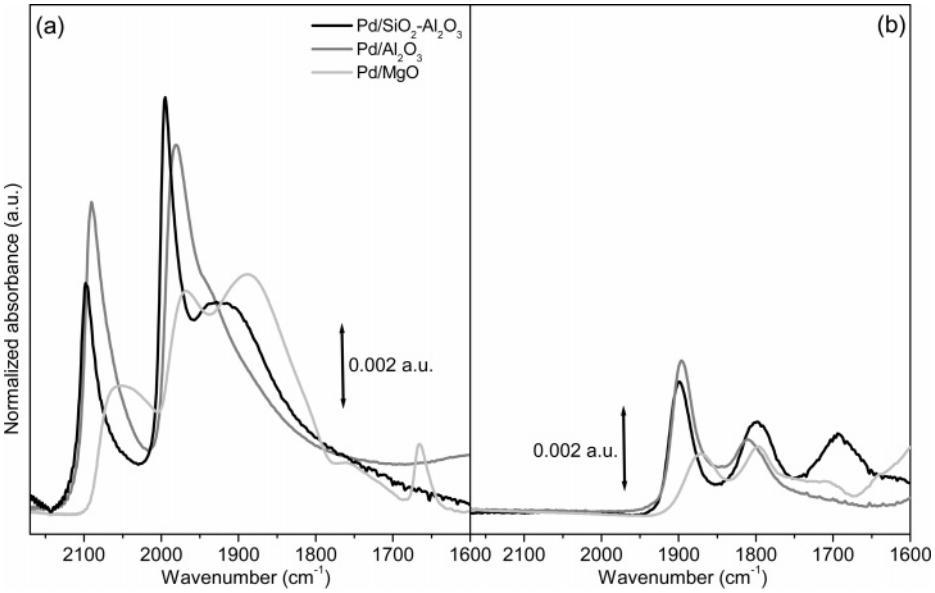

Figure 6. Comparison between the carbonyls features at θ_{max} (part a) and at θ_{min} (part b) on different Pd-supported systems: Pd/SiO_2−Al_2O_3 (black curve), Pd/Al_2O_3 (gray curve), and Pd/MgO (light gray curve). The vertical axis reports the absorbance normalized to the optical thickness of the samples.

the presence of chlorine results in an increased acidity of the support.[60−62] Concerning the modification induced by the chlorine residues on the electron transfer ability of the Pd nanoparticles, a withdraw of electron density from the palladium particles is expected, causing a decrease back-donation into the adsorbed CO and thus a relatively higher C−O stretching frequency.[10,32,33]

4. Conclusions

This work illustrates that the gap between the single crystals and the nanoparticles systems can be bridged, also in the case of Pd metal particles supported on high surface area inorganic oxides. The comparison with surface science results, in fact, allowed us to assign the whole set of bands appearing in the complex IR spectra of CO adsorbed on $Pd/SiO_2-Al_2O_3$, Pd/Al_2O_3, and Pd/MgO in terms of both carbonyl type (linear, two-, and threefold bridged) and of adsorbing surface (Pd(100) and Pd(111) faces). Also the presence of defective sites, typical of metal nanoparticles, has been considered. Finally, the role of the support in influencing the spectral features of carbonyls formed on Pd particles is clearly demonstrated: in particular, the more basic the oxygens of the support are, the higher the electron density that is added to the Pd particles. This phenomenon has strong effects in determining the CO stretching frequencies of both linear and bridged carbonyls.

Acknowledgment. We are indebted to Prof. G. Spoto for the friendly and important support during the TEM investigation.

References and Notes

(1) Xu, X. P.; Goodman, D. W. *J. Phys. Chem.* **1993**, *97*, 7711−7718.
(2) Xu, X. P.; Chen, P. J.; Goodman, D. W. *J. Phys. Chem.* **1994**, *98*, 9242−9246.
(3) Freund, H. J. *Angew. Chem., Int. Ed. Engl.* **1997**, *36*, 452−475.
(4) Wolter, K.; Seiferth, O.; Libuda, J.; Kuhlenbeck, H.; Baumer, M.; Freund, H. J. *Chem. Phys. Lett.* **1997**, *277*, 513−520.
(5) Wolter, K.; Seiferth, O.; Libuda, J.; Kuhlenbeck, H.; Baumer, M.; Freund, H. J. *Surf. Sci.* **1998**, *404*, 428−432.
(6) Henry, C. R. *Surf. Sci. Rep.* **1998**, *31*, 235−325.
(7) Surnev, S.; Sock, M.; Ramsey, M. G.; Netzer, F. P.; Wiklund, M.; Borg, M.; Andersen, J. N. *Surf. Sci.* **2000**, *470*, 171−185.
(8) Freund, H. J.; Baumer, M.; Kuhlenbeck, H. *Adv. Catal.* **2000**, *45*, 333−384.
(9) Sheppard, N.; De La Cruz, C. *Catal. Today* **2001**, *70*, 3−13.
(10) Bertarione, S.; Scarano, D.; Zecchina, A.; Johanek, V.; Hoffmann, J.; Schauermann, S.; Frank, M. M.; Libuda, J.; Rupprechter, G.; Freund, H. J. *J. Phys. Chem. B* **2004**, *108*, 3603−3613.
(11) Ozensoy, E.; Goodman, D. W. *Phys. Chem. Chem. Phys.* **2004**, *6*, 3765−3778.
(12) Xu, C.; Goodman, D. W. Ultrathin oxide films: model catalyst supports. In *Handbook of Heterogeneous Catalysis;* Ertl, G., Knözinger, H., Weitkamp, J., Eds.; Wiley-VCH: Weinheim, Germany, 1997; Vol. 2, pp 826−838.
(13) Henrich, V. E. *Rep. Prog. Phys.* **1985**, *48*, 1481−1542.
(14) Henrich, V. E.; Cox, P. A. *The Surface Science of Metal Oxides;* Cambridge University Press: Cambridge, U.K. 1994.
(15) Barteau, M. A. *Chem. Rev.* **1996**, *96*, 1413−1430.
(16) Barteau, M. A.; Vohs, J. M. Oxide model systems. In *Handbook of Heterogeneous Catalysis;* Ertl, G., Knözinger, H., Weitkamp, J., Eds.; Wiley-VCH: Weinheim, Germany, 1997; Vol. 2, pp 873−888.
(17) Lear, T.; Marshall, R.; Gibson, E. K.; Schutt, T.; Klapotke, T. M.; Rupprechter, G.; Freund, H. J.; Winfield, J. M.; Lennon, D. *Phys. Chem. Chem. Phys.* **2005**, *7*, 565−567.
(18) Lavalley, J. C. *Catal. Today* **1996**, *27*, 377−401.
(19) Morterra, C.; Magnacca, G. *Catal. Today* **1996**, *27*, 497−532.
(20) Knözinger, H. Infrared spectroscopy for the characterization of surface acidity and basicity. In *Handbook of Heterogeneous Catalysis;* Ertl, G., Knözinger, H., Weitkamp, J., Eds.; Wiley-VCH: Weinheim, Germany, 1997; Vol. 2, pp 707−732.
(21) Zecchina, A.; Arean, C. O. *Catal. Rev.−Sci. Eng.* **1993**, *35*, 261−317.
(22) Zecchina, A.; Lamberti, C.; Bordiga, S. *Catal. Today* **1998**, *41*, 169−177.
(23) Zecchina, A.; Scarano, D.; Bordiga, S.; Spoto, G.; Lamberti, C. *Adv. Catal.* **2001**, *46*, 265−397.
(24) Spoto, G.; Gribov, E. N.; Ricchiardi, G.; Damin, A.; Scarano, D.; Bordiga, S.; Lamberti, C.; Zecchina, A. *Prog. Surf. Sci.* **2004**, *76*, 71−146.
(25) van der Eerden, A. M. J.; Visser, T.; Nijhuis, A.; Ikeda, Y.; Lepage, M.; Koningsberger, D. C.; Weckhuysen, B. M. *J. Am. Chem. Soc.* **2005**, *127*, 3272−3273.
(26) Seiferth, O.; Wolter, K.; Dillmann, B.; Klivenyi, G.; Freund, H.-J.; Scarano, D.; Zecchina, A. *Surf. Sci.* **1999**, *421*, 176−190.
(27) Escalona Platero, E.; Fubini, B.; Zecchina, A. *Surf. Sci.* **1987**, *179*, 404−424.
(28) (a) Spoto, G.; Gribov, E.; Damin, A.; Ricchiardi, G.; Zecchina, A. *Surf. Sci.* **2003**, *540*, L605−L610. (b) Gribov, E. N.; Bertarione, S.; Scarano, D.; Lamberti, C.; Spoto, G.; Zecchina, A. *J. Phys. Chem. B* **2004**, *108*, 16174−16186.
(29) Blaser, H. U.; Indolese, A.; Schnyder, A.; Steiner, H.; Studer, M. *J. Mol. Catal. A***2001**, *173*, 3−18.
(30) Scirè, S.; Minicò, S.; Crisafulli, C. *Appl. Catal. A* **2002**, *235*, 21−31.
(31) Santacesaria, E.; Wilkinson, P.; Babini, P.; Carrà, S. *Ind. Eng. Chem. Res.* **1988**, *27*, 780−784.
(32) Lear, T.; Marshall, R.; Lopez-Sanchez, J. A.; Jackson, S. D.; Klapotke, T. M.; Baumer, M.; Rupprechter, G.; Freund, H. J.; Lennon, D. *J. Chem. Phys.* **2005**, *123*, article no. 174706.
(33) Lear, T.; Marshall, R.; Lopez-Sanchez, J. A.; Jackson, S. D.; Klapotke, T. M.; Baumer, M.; Rupprechter, G.; Freund, H. J.; Lennon, D. *J. Chem. Phys.* **2006**, *124*, article no. 069901.
(34) Rose, M. K.; Mitsui, T.; Dunphy, J.; Borg, A.; Ogletree, D. F.; Salmeron, M.; Sautet, P. *Surf. Sci.* **2002**, *512*, 48−60.
(35) Sheppard, N.; Nguyen, T. T. *Adv. IR Raman Spectrosc.* **1978**, *5*, 67−148.
(36) Delacruz, C.; Sheppard, N. *J. Mol. Struct.* **1990**, *224*, 141−161.
(37) Bolis, V.; Barbaglia, A.; Bordiga, S.; Lamberti, C.; Zecchina, A. *J. Phys. Chem. B* **2004**, *108*, 9970−9983.
(38) Lupinetti, A. J.; Strauss, S. H.; Frenking, G. *Prog. Inorg. Chem.* **2001**, *49*, 1−112.
(39) Strauss, S. H. *J. Chem. Soc., Dalton Trans.* **2000**, 1−6.
(40) Hoffmann, F. M. *Surf. Sci. Rep.* **1983**, *3*, 107−192.
(41) Kuhn, W. K.; Szanyi, J.; Goodman, D. W. *Surf. Sci.* **1992**, *274*, L611−L618.
(42) Szanyi, J.; Kuhn, W. K.; Goodman, D. W. *J. Vac. Sci. Technol. A* **1993**, *11*, 1969−1974.
(43) Giessel, T.; Schaff, O.; Hirschmugl, C. J.; Fernandez, V.; Schindler, K. M.; Theobald, A.; Bao, S.; Lindsay, R.; Berndt, W.; Bradshaw, A. M.; Baddeley, C.; Lee, A. F.; Lambert, R. M.; Woodruff, D. P. *Surf. Sci.* **1998**, *406*, 90−102.
(44) Ortega, A.; Huffman, A.; Bradshaw, A. M. *Surf. Sci.* **1982**, *119*, 79−94.
(45) Hollins, P. *Surf. Sci. Rep.* **1992**, *16*, 51−94.
(46) Hollins, P.; Pritchard, J. *Prog. Surf. Sci.* **1985**, *19*, 275−349.
(47) Busca, G.; Lorenzelli, V. *Mater. Chem.* **1982**, *7*, 89−126.
(48) Maciejewski, M.; Baiker, A. *J. Phys. Chem.* **1994**, *98*, 285−290.
(49) Liotta, L. F.; Martin, G. A.; Deganello, G. *J. Catal.* **1996**, *164*, 322−333.
(50) Note that by dosing CO_2 at 300 K on the $Pd/SiO_2-Al_2O_3$ sample, an intense and quite broad band appears in the IR spectrum around 1700 cm^{-1}, which (in this case) can be assigned in a straightforward way to the carbonate species. Opposite to what was observed for the band at 1694 cm^{-1}, this component is stable upon the successive dosage of CO.
(51) Horwitz, C. P.; Shriver, D. F. *Adv. Organomet. Chem.* **1984**, *23*, 219−305.
(52) Guglielminotti, E. *Langmuir* **1986**, *2*, 812−820.
(53) Zecchina, A.; Escalona Platero, E.; Otero Arean, C. *Inorg. Chem.* **1988**, *27*, 102−106.
(54) Alich, A.; Nelson, N. J.; Strope, D.; Shkiver, D. F. *Inorg. Chem.* **1972**, *11*, 2976−2983.
(55) Kristoff, J. S.; Shriver, D. F. *Inorg. Chem.* **1974**, *13*, 499−506.
(56) Guglielminotti, E. *J. Catal.* **1989**, *120*, 287−291.
(57) Babaeva, M. A.; Bystrov, D. S.; Kovalgin, A. Y.; Tsyganenko, A. A. *J. Catal.* **1990**, *123*, 396−416.
(58) Zecchina, A.; Coluccia, S.; Spoto, G.; Scarano, D.; Marchese, L. *J. Chem. Soc., Faraday Trans.* **1990**, *86*, 703−709.
(59) Mojet, B. L.; Miller, J. T.; Koningsberger, D. C. *J. Phys. Chem. B* **1999**, *103*, 2724−2734.
(60) Leofanti, G.; Padovan, M.; Garilli, M.; Carmello, D.; Zecchina, A.; Spoto, G.; Bordiga, S.; Palomino, G. T.; Lamberti, C. *J. Catal.* **2000**, *189*, 91−104.
(61) Leofanti, G.; Padovan, M.; Garilli, M.; Carmello, D.; Marra, G. L.; Zecchina, A.; Spoto, G.; Bordiga, S.; Lamberti, C. *J. Catal.* **2000**, *189*, 105−116.
(62) Leofanti, G.; Marsella, A.; Cremaschi, B.; Garilli, M.; Zecchina, A.; Spoto, G.; Bordiga, S.; Fisicaro, P.; Berlier, G.; Prestipino, C.; Casali, G.; Lamberti, C. *J. Catal.* **2001**, *202*, 279−295.